Transient Kinetics during the Isothermal Reduction of NO by CO on Rh(111) As Studied with Effusive Collimated Molecular Beams†

Chinnakonda S. Gopinath and Francisco Zaera*

Department of Chemistry, University of California, Riverside, California 92521

Received: September 1, 1999; In Final Form: January 10, 2000

The transient kinetics of the reaction between NO and CO on clean Rh(111) surfaces have been studied using molecular beams in conjunction with mass spectrometry detection. The changes in the partial pressures of the reactants (CO and NO) and products (N_2 and CO_2) as a function of time have been used as a measure of the evolution of the uptake and desorption rates, respectively, for temperatures between 350 and 1000 K and for NO:CO mixture ratios between 4:1 and 1:99. Post-mortem temperature programmed desorption (TPD) and CO titration experiments were also performed in order to estimate the surface coverages of atomic nitrogen and oxygen left on the Rh(111) surface by the gas mixture. Systematic variations were observed during the transition from the clean surface to the steady-state catalytic regime that correlate well with the overall reaction rates in the latter. Specifically, there is a time delay in the production of molecular nitrogen because of the need to build up a threshold atomic nitrogen coverage on the surface before the start of the desorption of N_2. This atomic nitrogen coverage, as calculated by the time delay in the transient, corresponds to that estimated by TPD after the reaction, and displays a dependence on the NO:CO ratio in the reaction mixture, increasing at a given temperature as the beam becomes richer in CO. Initial sticking coefficients were also determined for both NO and CO in NO + CO mixtures as a function of surface temperature and beam composition.

1. Introduction

A fresh solid catalyst usually undergoes substantial changes at the onset of a catalytic reaction, before it reaches its steady-state condition. Adsorbate-induced chemical and structural changes are among the key reasons invoked to explain these initial changes, but the buildup of the appropriate layers of adsorbates on the surface might also affect the steady-state kinetics in more subtle ways. Consequently, the transient behavior of a catalytic system can often provide valuable information about its performance under steady-state conditions. The reduction of NO by CO on rhodium surfaces in particular displays some chemical changes at the onset of the reaction that become evident by differences in rates of production of N_2 and CO_2 during the first few seconds of the process. Although there have already been a few reports on both the transient and the steady-state behavior of NO + CO and NO + H_2 mixtures on rhodium catalysts,[1−35] there have not been, to the best of our knowledge, any careful studies on the correlation between the two. The present report addresses this very issue, and relates the transient behavior to the knowledge previously acquired in our ongoing study on the details of the kinetics and mechanism of NO reduction on Rh(111) single crystals.[3−6]

Kinetic results from initial transient studies in isothermal experiments with NO + CO molecular beams as they impinge on a clean Rh(111) single-crystal surface are presented below. The experiments were conducted over a wide range of conditions, including temperatures between 350 and 1000 K and NO:CO gas mixture ratios between 4:1 and 1:99. It was found that the need for the buildup of a layer of atomic surface nitrogen before the beginning of the N_2 production step identified before[5,6] is manifested in the transient by a delay in the production of molecular nitrogen after the start of the reaction. The value of this threshold nitrogen coverage needed to initiate the N_2 production is sensitive to the composition of the reaction mixture, and increases systematically at a given temperature as the beam becomes richer in CO. A correlation between the rates in the transient and the steady-state regimes was also identified in terms of the NO uptake at the onset of the reaction. Maximum rates are observed during the steady-state conversion of the NO + CO mixture when the transient is short and does not deviate much from the subsequent kinetic behavior of the system; this typically happens with close-to-stoichiometric mixtures. There is also a synergistic effect between beam composition and temperature by which beams with lower NO:CO ratios require higher temperatures to maximize their reaction rates.

2. Experimental Section

All of the experiments reported here were performed in a 6.0-L stainless-steel UHV chamber evacuated with a 170-L/s turbo-molecular pump to a base pressure of about 2×10^{-10} Torr, as described in detail elsewhere.[36,37] Briefly, this system is equipped with a UTI 100C quadrupole mass spectrometer, a sputtering ion gun, and a molecular beam doser. The doser, a 1.2-cm-diameter array of parallel microcapillary glass tubes 10 μm in diameter and 2 mm in length aimed directly at the surface, is connected to a calibrated volume via leak and shutoff valves. The beam flux is set by filling the back volume to a specific pressure, as measured by a MKS Baratron gauge, and by adjusting the leak valve to a predetermined set point. A constant total flux of 0.50 monolayer per second (ML/s) was used in all of the experiments reported here unless otherwise specified. A movable stainless-steel flag is placed between the surface and the doser in order to intercept the beam at will.

The solid sample, an approximately rectangular (1.10×0.56 cm^2) Rh(111) single crystal, was cleaned in situ, initially by

† Part of the special issue "Gabor Somorjai Festschrift".

* Corresponding author.

10.1021/jp993103g CCC: $19.00
Published on Web 02/18/2000

Ar^+ sputtering and before each experiment by cycles of oxygen treatments (1×10^{-7} Torr at 900 K for up to 20 min) and annealing to 1200 K, until reproduction of the NO temperature programmed desorption (TPD) spectra reported in the literature was achieved. The crystal could be heated resistively or cooled with a liquid-nitrogen reservoir to any temperature between 90 and 1200 K, and was placed at a distance of 0.5 cm from the front of the doser to ensure a reasonably flat gas-flux profile.[36] In our arrangement, the sample intercepts only about 20% of the total beam, but the contribution from the background to the measurements of the reaction rates was nevertheless deemed by independent calibration experiments to be less than 20% of that from the direct beam.[36] The surface temperature was monitored continuously by using a chromel−alumel thermocouple spot-welded to the back of the crystal, and was kept constant during the kinetic runs with a homemade precision temperature controller. TPD spectra were recorded at a constant heating rate of 10 K/s. Isotopically labeled ^{15}NO (CIL, 98% ^{15}N purity) and unlabeled CO (Matheson, 99.9% purity) were used as supplied. The pressures of the gases in the vacuum chamber were measured with a nude ion gauge. Pressures were calibrated for differences in ionization sensitivities by comparison with the original composition of the NO + CO beams, as measured with the Baratron pressure gauge.[38]

The time evolution of the partial pressures of up to 10 different species, including N_2O and NO_2, was followed simultaneously both in the isothermal kinetic runs and in the TPD experiments by using the computer-controlled quadrupole mass spectrometer, which was placed out of the line of sight of both the beam and the crystal in order to avoid any artifacts due to possible angular profiles in either the scattered or the desorbing gases. The raw kinetic data in Figures 2, 3, and 8 are reported in arbitrary mass spectrometer units, but calibration bars are included in those plots for relative comparisons. The absolute sticking coefficients, rates, and coverages reported in Figures 5−7 and 10−14 were estimated by independent calibration of the mass spectrometer signals for nitric oxide, nitrogen, and carbon monoxide, as described elsewhere.[3−6] Because only ^{15}N-labeled nitric oxide was used in this work, ^{15}NO, $^{15}N_2$, and ^{15}N will be simply referred to as NO, N_2, and N, respectively, hereafter.

3. Results

3.1. General Considerations. The isothermal kinetic runs reported here for the (NO + CO)/Rh(111) system were carried out by following a procedure explained in detail in our previous publications.[3−6,36,37,39] The clean rhodium surface is first heated to a preset constant temperature, and then exposed to an effusive collimated molecular beam with a specific NO:CO ratio while the partial pressures of the different gases of interest are followed by mass spectrometry as a function of time. Figure 1 shows typical raw kinetic data obtained in this way. In this case the data represent the time evolution of the partial pressures of CO, NO, N_2, and CO_2 for a 1:1 NO:CO beam, a total flux of 0.15 ML/s, and a reaction temperature of 475 K. The flag is first placed in the intercepting position so the crystal is not exposed directly to the beam when the NO + CO molecular beam is turned on (at time $t = 10$ s in Figure 1), but it is removed soon thereafter (at $t = 20$ s) to initiate the kinetic measurements. The evolution of the partial pressures of the different gases from the point of flag removal until the steady state is reached (about 30 s later, at $t = 50$ s) is the focus of this work. Because of the high pumping speed for most gases (all but NO, see below) in the vacuum chamber, these changes in partial pressures are directly related to the corresponding uptake and desorption rates.

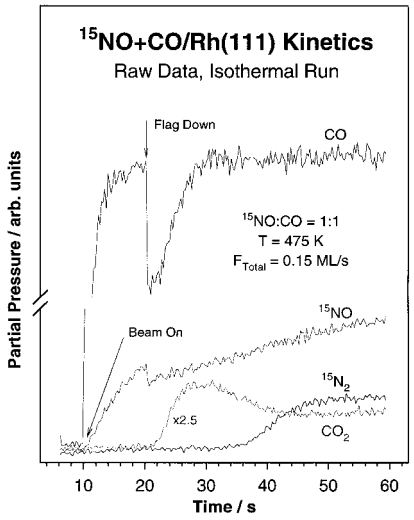

Figure 1. Typical transient raw data from an isothermal kinetic run of the type described in this report. An effusive collimated ^{15}NO + CO molecular beam (1:1 ^{15}NO:CO in this example) is directed onto a clean rhodium (111) surface kept at a constant temperature (475 K) as the partial pressures of both reactants (^{15}NO and CO) and products ($^{15}N_2$ and CO_2) are followed in time. Note the difference between the instantaneous evolution of CO_2 at the flag-down point and the delay (by about 15 s) before the start of the evolution of N_2.

A few minor points must be made here before addressing the main results of this study. First, note that within the first 10 s of the experiment, between the times when the molecular beam is turned on and the flag is removed from its path, there is some adsorption of NO and CO from the background. As a result, the surface is already covered with some adsorbates at the beginning of the kinetic run. The fact that the surface is not completely clean at the point of flag removal is particularly important for understanding some of the initial sticking-coefficient data (see below). Second, it is also worthwhile to notice that the NO partial pressure rises continuously during the isothermal runs because of the somewhat limited pumping speed of the system for that molecule. This factor can be taken into account in the data analysis, and does not represent a major obstacle in understanding the chemistry of NO + CO on the rhodium surface. Last, it should be highlighted that the trace for $^{15}N_2O$ (46 amu) shows no features anywhere during the kinetic runs, indicating that no N_2O is produced at any stage of the experiments reported in this paper; no more will be said about this species.

3.2. Temperature Dependence. Figure 2 displays the time evolution of the transient rates of desorption for CO_2 (a, left panel) and N_2 (b, right panel) during the exposure of the Rh(111) surface to a 1:3 NO:CO beam at different crystal temperatures. These data indicate that no significant NO conversion can be catalytically sustained at temperatures below 400 K. Although there is a noticeable rise in the partial pressure of CO_2 right after the flag is removed in the runs between 375 and 400 K, that initial CO_2 evolution dies down quickly thereafter (there is no change in the CO_2 partial pressure when the beam is blocked at later times).[4] In the case of N_2, no significant production is observed in either the transient or the steady-state regimes; the signal measured in the $^{15}N_2$ (30 amu) traces below 400 K in the right panel of Figure 2 is exclusively due to the 2% unlabeled ^{14}NO contamination in the ^{15}NO gas. Previous TPD results from surfaces exposed to NO + CO mixtures have indicated that, indeed, desorption of N-containing species starts only at temperatures above 400 K.[3,14,15]

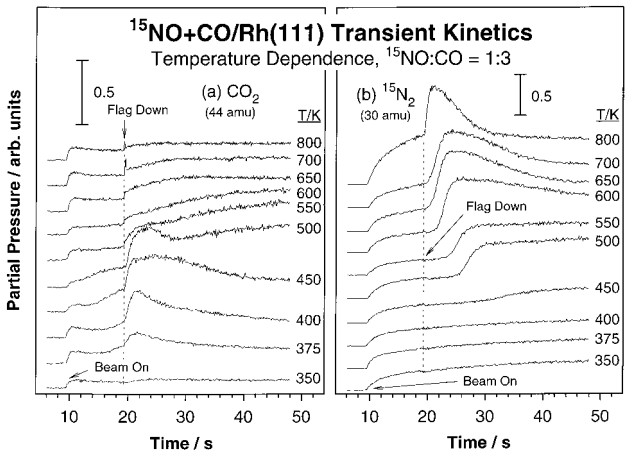

Figure 2. Time evolution of the partial pressures of the products CO_2 (a, left) and $^{15}N_2$ (b, right) during the transient of kinetic experiments such as that described in Figure 1 as a function of surface temperature. The ^{15}NO:CO ratio in this figure is 1:3 in all runs. CO_2 production below 400 K is seen only in the transient state. The overall NO + CO steady-state rate increases above 450 K, and the transient behavior becomes optimum (fast steady-state approach and minimum rate overshooting) between 550 and 600 K. Excess nitrogen is produced in the transient above 600 K.

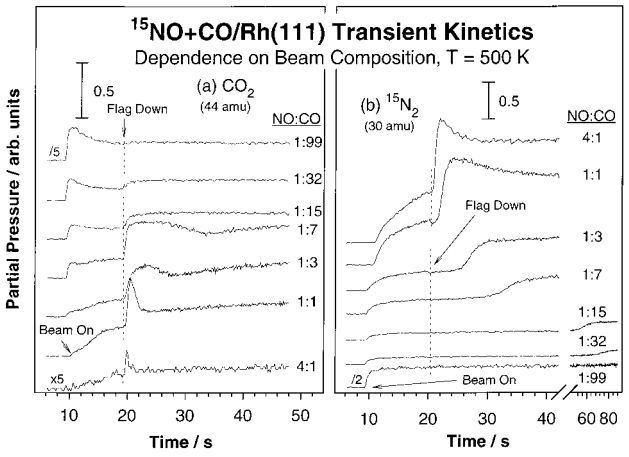

Figure 3. Time evolution of the partial pressures of the products CO_2 (a, left), and $^{15}N_2$ (b, right) during kinetic experiments such as those described in Figures 1 and 2 at 500 K as a function of NO:CO beam compositions. Again, optimum transient behavior is seen for mixtures with NO:CO ratios between 1:1 and 1:3.

An increase in reactivity is seen in Figure 2 above 450 K, as indicated by the clear changes in the partial-pressure traces of both N_2 and CO_2 as the flag is removed from the path of the beam. Notice, however, that N_2 production is seen only after a delay which ranges from about 14 s at 450 K to less than 1 s above 650 K. Also, below 600 K, the N_2 desorption rates approach their steady-state values asymptotically, but above that temperature there is an overproduction of N_2 in the first 10 s or so, before the steady-state regime is reached. A similar overproduction of N_2, albeit less pronounced, is observed when the beam is blocked during the steady-state conditions.[4,5] In contrast to the N_2 behavior, the response of the CO_2 traces to the exposure of the surface to the beam is immediate at all temperatures, and it is more acute between 450 and 500 K, where CO_2 production overshoots within the first few seconds of the kinetic run. The excess CO_2 transient disappears above 550 K, and by 650 K the formation of CO_2 slows drastically. It is important to point out that it is between 550 and 600 K, where both N_2 and CO_2 reach their steady-state levels quickly and asymptotically, that the maximum overall NO + CO reaction rate is attained in the steady state.[4]

One more important feature to be highlighted from the data in Figure 2 is the dip in the CO_2 rate observed in the 500 K case about 8 s after flag removal. A similar behavior was observed by Comelli and co-workers[10,40] on Rh(110), and was attributed to surface structural modifications as observed by low-energy electron diffraction (LEED). Comparable features were observed in our study between 450 and 550 K for other beam compositions.

3.3. Composition Dependence. Figure 3 displays the kinetic traces obtained for CO_2 and N_2 during the transient of the NO + CO reaction at a constant temperature, 500 K, for NO:CO ratios ranging from 4:1 to 1:99. Note here that when the beam is rich in either NO (for instance, in the case of the 4:1 NO:CO composition) or CO (in the 1:99 NO:CO case), the rate of CO_2 production is low. This is in fact true at all surface temperatures, even those high enough to dissociate NO molecules. However, in going from CO-rich beams to beams with higher NO concentrations, a rapid increase is detected in the NO + CO transient (as well as steady-state) CO_2 and N_2 desorption rates, until a maximum is reached at an approximately equimolar NO:CO composition. The rate of CO_2 formation always responds almost immediately to the changes in the beam, but the N_2 rate response is fast only with NO-rich beams; with CO-rich beams, time delays in N_2 production such as those mentioned before are observed. At 500 K this delay increases from 7 s for a 1:3 NO:CO composition to 50 s for a 1:32 beam, and with a 1:99 composition no N_2 production can be seen at all within the experimental dosing time of 200 s. Finally, a dip in the CO_2 production rate can again be seen in the left panel of Figure 3 about 3−15 s after the initial flag removal for the 1:1, 1:3, and 1:7 NO:CO compositions; its actual start shifts to later times and its width increases with increasing concentration of CO in the beam.

A more systematic study of the transient behavior of the NO + CO reaction on Rh(111) was carried out as a function of both beam composition and temperature. A few interesting points are worth highlighting from the resulting data. (1) For a given NO:CO beam composition, there is an optimum reaction temperature in terms of the transient behavior, somewhere between 450 and 850 K, for which the responses are fast and there is no obvious overproduction of either N_2 or CO_2. At 500 K, this occurs for a NO:CO ratio somewhere between 1:1 and 1:3 (Figure 3). (2) This optimum temperature shifts to higher temperature with increasing CO (and/or decreasing NO) content in the reaction mixture, an indication that there is a synergy between the reaction temperature and the beam composition in terms of their effect on the transient kinetics of the NO + CO reaction. Figure 4 displays these changes in optimum beam compositions as a function of temperature in an Arrhenius fashion in order to highlight the activated nature of this phenomenon (see later). (3) There is also an optimum condition in terms of NO:CO ratios and temperatures, somewhere between 1:1 and 1:3 and between 500 and 550 K, respectively, which maximizes the reaction rate. (4) Finally, the observations in the transient parallel the behavior previously reported for the steady-state rates.[4] All of these results demonstrate that the reaction rates, which depend on surface coverages, are effectively controlled by both the surface temperature and the beam composition. It appears that the effect of increasing the reaction temperature can be compensated to some extent by an increase in the concentration of CO in the beam.

3.4. NO and CO Initial Adsorption Coefficients. Previous studies have determined that NO adsorption on Rh(111) surfaces

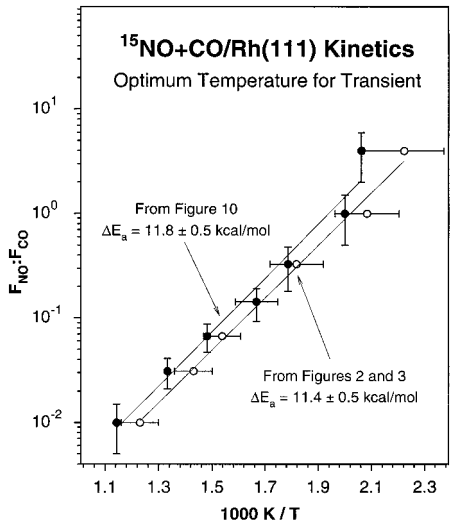

Figure 4. Arrhenius display of the beam compositions required for optimum transient behavior as a function of reaction temperature. Two independent sets of data are shown here: one obtained by direct observation of raw kinetic data such as those in Figures 2 and 3 (open circles) and another from estimates using the nitrogen-coverage differential parameter ($\Delta\Theta_N^{Trans}$) defined in Figure 9 (filled circles). The Arrhenius behavior shown here reflects an approximately 11.5 kcal/mol difference in adsorption energy between NO and CO under reaction conditions.

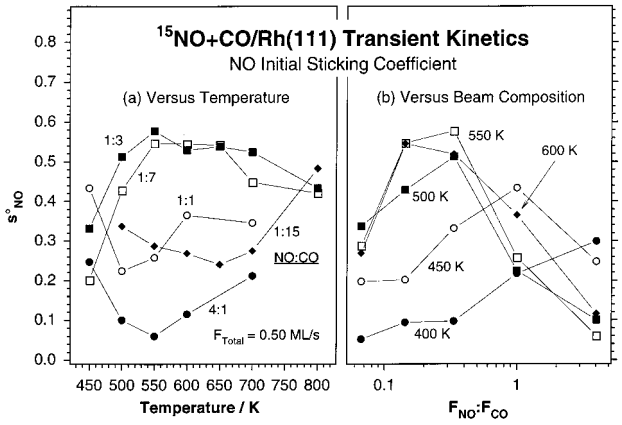

Figure 5. Initial sticking coefficient ($s°_{NO}$) for the adsorption of NO from NO + CO beams on an Rh(111) surface as a function of surface temperature (a, left) and beam composition (b, right). The total flux of the reactants was kept constant in all of these experiments at F_{Total} = 0.50 ML/s. The value of $s°_{NO}$ generally goes through a maximum at the conditions required for optimum surface stoichiometric NO and CO coverages.

is dissociative at temperatures above room temperature[19,28] and that it displays high sticking coefficients, on the order of 0.7−0.8.[3] The uptake kinetics for NO, however, do change somewhat in the presence of CO. Figure 5 displays the dependence of the NO initial sticking coefficient ($s°_{NO}$) on both temperature and beam composition; the left panel shows $s°_{NO}$ versus reaction temperature for a number of NO:CO ratios, while the right panel displays $s°_{NO}$ versus NO:CO ratio for several temperatures. Notice that although the total flux intensity, F_{Total}, was kept constant at 0.50 ML/s in all of these experiments, F_{NO} and F_{CO} both change with beam composition. The initial sticking coefficients were calculated from the drop in NO partial pressure at the flag-removal point of the transient, as described in previous publications[36,39] (the NO and CO traces display sharp drops at the flag-removal point, the depths of which reflect the corresponding sticking coefficients; see, for instance, the data

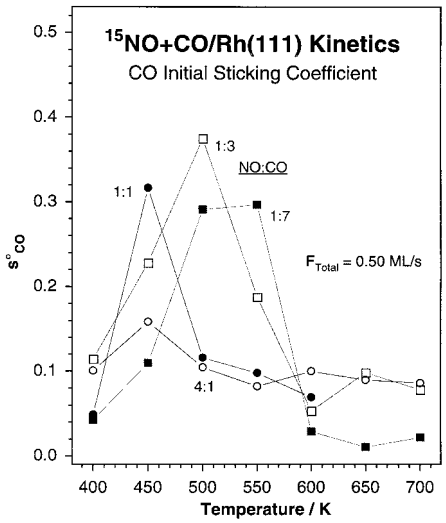

Figure 6. Initial sticking coefficient ($s°_{CO}$) for the adsorption of CO from NO + CO beams on an Rh(111) surface as a function of surface temperature for a number of beam compositions. The value of $s°_{CO}$ generally decreases at lower temperatures than $s°_{NO}$.

in Figure 1). It is worth recalling again that these values for $s°_{NO}$ are not true initial sticking coefficients on the clean surface, but only approximations because of the adsorption from background gases that occurs before the unblocking of the beam. The data in Figure 5 indicate that, for NO:CO compositions near the stoichiometric ratio, $s°_{NO}$ increases with increasing temperature, reaches a broad maximum somewhere between 550 and 700 K, and decreases afterward. With NO-rich beams, however, $s°_{NO}$ actually decreases from 400 to 550 K before rising again at higher temperatures and displays relatively low values in all cases. A similar behavior is also seen with CO-rich compositions, except that the minimum in $s°_{NO}$ shifts to higher temperatures (higher as more CO is added to the beam). In terms of the dependence of $s°_{NO}$ on beam composition at a given temperature, an initial increase with increasing fraction of NO in the beam is observed in all cases, as expected. This rise is faster and reaches a maximum with lower NO:CO ratios at higher temperatures, and $s°_{NO}$ actually drops in the presence of excess NO above about 500 K. Absolute maxima in $s°_{NO}$ values slightly above 0.5 are seen around 550−650 K for NO:CO ratios between 1:3 and 1:7. These are the same conditions for which maximum steady-state rates are seen.

Figure 6 displays a similar dependence plot of the initial sticking coefficient for CO ($s°_{CO}$) on temperature for a few beam compositions. Again, in general, $s°_{CO}$ first increases with temperature to a maximum value, roughly following the trends seen for $s°_{NO}$ in Figure 5, except that the drop that follows starts at lower temperatures. The maximum in $s°_{CO}$ shifts to higher temperature with increasing CO content in the beam, and is the highest (about 0.4) for a 1:3 NO:CO ratio at 500 K. It is important to point out, however, that the $s°_{CO}$ in this figure might be underestimated in some cases because of the fast competition between CO and NO adsorption. In fact, the initial drop in CO pressure that is seen right after the removal of the flag from the path of the beam is, in many cases, followed soon thereafter by a sharp increase above the final steady-state level, indicating the displacement of some adsorbed CO by NO. This displacement is explored in more detail in the next section.

To better highlight the effect of the initial sticking coefficients of NO and CO on the overall steady-state reaction rates (R_{ss}), Figure 7 shows the ratios of those steady-state NO + CO conversion rates to the initial NO ($s°_{NO}$, left panel) and CO ($s°_{CO}$,

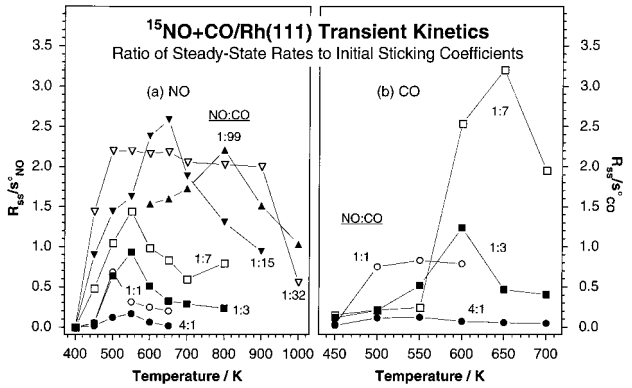

Figure 7. Steady-state-to-transient uptake ratios for NO (a, left panel) and CO (b, right panel) in the (NO + CO)/Rh(111) beam experiments reported here as a function of reaction temperature for a number of beam compositions. The NO uptake in the steady state (R_{ss}) is higher than in the transient state ($s°_{NO}$) for CO-rich beams, and often reaches maximum values for the same conditions for which maxima are seen in the steady-state rates. There is also a general increase in the ratio $R_{ss}/s°_{CO}$ with increasing reaction temperature.

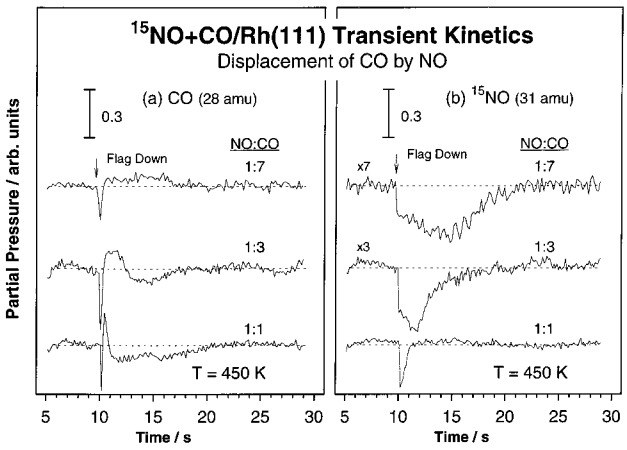

Figure 8. Typical transient behavior for cases in which CO is displaced by NO. Data are shown for the time evolution of CO (a, left) and NO (b, right) for three beam compositions, all at $T = 450$ K and $F_{Total} = 0.50$ ML/s. The displacement is manifested here by the desorption (pressure increase) of CO soon after the flag is removed from the path of the beam ($t = 10$ s). This CO displacement is mainly observed between 400 and 500 K for most beam compositions, but it is also visible at high temperatures in some specific cases.

right panel) sticking coefficients as a function of temperature for a number of beam compositions. Reasonably clear trends with $s°_{NO}$ can be seen in the left panel. For instance, for a given NO:CO beam composition, the $R_{ss}/s°_{NO}$ ratio first increases with temperature but then reaches a maximum and decreases again, a behavior that parallels that previously reported for the absolute values of the NO + CO conversion rate under the steady state.[4] Notice also that the $R_{ss}/s°_{NO}$ maximum shifts to higher temperature with increasing CO content in the beam, from approximately 500 K for the 1:1 NO:CO mixture to about 800 K for the 1:99 case. Because $s°_{NO}$ does not vary significantly with changing reaction conditions, at least for intermediate temperatures and beam compositions, it can be concluded that $s°_{NO}$ does not influence the overall rate much. In contrast, the values of the $R_{ss}/s°_{NO}$ ratio continue to increase steadily with increasing CO concentration in CO-rich beams, long past the point at which the steady-state rates drop significantly.[4] In fact, as the beam becomes richer in CO, the NO steady-state-to-transient uptake ratio increases to values above 1, most likely because the NO sticking coefficient is quite low at the beginning of the runs under those conditions but increases as soon as some CO is displaced from the surface. In other words, with CO-rich beams, the surface in the transient is covered with excess CO, and NO adsorption is inhibited, but as the steady state is approached, a surface NO:CO coverage ratio closer to stoichiometry is reached. This effect generally increases and spreads toward higher temperatures with increasing CO concentration in the beam. A maximum is also seen in the value of $R_{ss}/s°_{CO}$ at the intermediate optimum reaction temperatures for a given beam composition (Figure 7, right frame).

3.5. Displacement of CO by NO. As mentioned before, chemisorbed CO can, under some conditions, be displaced by NO. The displacement of adsorbed species by molecules from the gas phase has been seen for a number of cases.[15,41−43] In the (NO + CO)/Rh(111) system studied here, this effect is most noticeable between 400 and 500 K. Figure 8 displays initial kinetic traces for CO (a, left) and NO (b, right) at 450 K with 1:1, 1:3, and 1:7 NO:CO beams. As in all other experiments, the molecular beam was turned on about 10 s before the removal of the flag from its path, so some background adsorption occured before the start of these measurements. A third-order polynomial background curve was subtracted from each of the traces of this figure in order to better highlight the pressure changes at the point of beam unblocking. The data for the adsorption of NO in Figure 8 follow the expected behavior, namely, they show an initial drop right at the point of flag removal because of the initial uptake, and a subsequent asymptotic approach to the steady state. The time evolution of the partial pressure of CO, on the other hand, is more complex, as the immediate drop that occurs upon the unblocking of the beam is soon followed by an increase past the final steady-state level. It appears that a large amount of CO desorbs from the surface at that point despite the continuous impingement of CO molecules from both the molecular beam and the background. This can be explained by the preferential and strong adsorption of NO on Rh(111), a preference that induces the displacement of some of the CO molecules already adsorbed on that surface. The data in Figure 8 also show that, as the beam becomes richer in CO, displacement of CO by NO requires longer times, perhaps because of the decrease in the absolute value of F_{NO}.

In terms of the effect of the surface temperature on this displacement, no CO displacement was seen here below 400 K, perhaps because of a lack of sensitivity in our mass spectrometer. A slow displacement of CO by NO was inferred in our earlier report[4] from data on the coverages of NO and CO that result after dosing NO + CO mixtures on Rh(111) at 350 K. For instance, near stoichiometric ratios of NO and CO (about 0.1 ML of each) are seen on the surface after dosing with a 1:7 NO:CO beam for 200 s, but no significant surface CO is detected when using a 1:1 mixture. No displacement was seen at high temperatures here either, except for the cases of the 1:1 and 1:7 NO:CO beam compositions at 700 and 800 K, respectively. However, the steady-state coverages of all adsorbates, NO and CO in particular, are always low above 700 K, so no significant displacement is expected under such conditions. It should also be mentioned that both the residence time of CO on the surface[4] and $s°_{NO}$[3] decrease with increasing temperature. All of these factors combine to make the potential high-temperature displacement of CO difficult to detect.

3.6. Coverages of Nitrogen and Oxygen on the Surface during the Reaction Transient. The connection between overall steady-state rates and surface nitrogen coverages in the transient is addressed next. Figure 9 illustrates the method used here to calculate the differences between the actual nitrogen

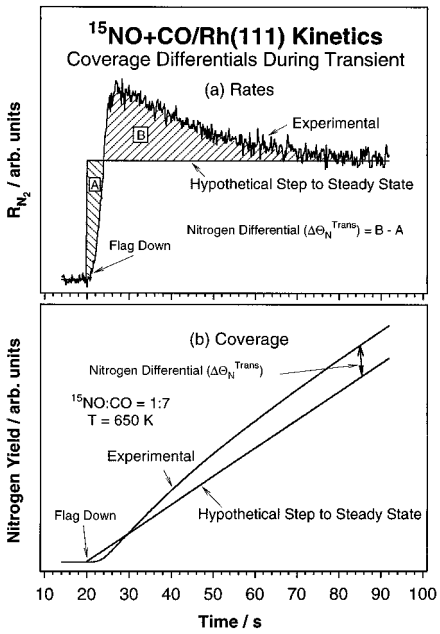

Figure 9. Illustration of the method used to calculate the differences between the surface coverages built up on the surface during the transient and those expected if the steady state were reached right after the unblocking of the beam. Top (a): Nitrogen desorption transient rates versus time. The shaded areas represent the differences in nitrogen coverage ($\Delta\Theta_N^{Trans}$) between the experimental data and a hypothetical step function representing the reaching of instant steady state at the point of flag removal. Bottom (b): N_2 yield versus time calculated by integration of the above traces.

(or CO_2) yields seen in the transient and those expected if the NO + CO reaction were to reach its steady state as soon as the flag was removed from the path of the beam. The top panel shows an example of the time evolution of the nitrogen production rate from the beginning of the direct exposure of the Rh(111) surface to the beam to a point at which the steady state is attained and, for contrast, the results that would be expected if R_{N_2} were to reach its steady-state value immediately after the removal of the flag (a step function). The bottom panel shows the time evolution of the nitrogen yield for both cases, obtained by integration of the data shown in the top panel. In both cases, the difference between the observed (experimental) and expected (hypothetical) yields is ascribed to a change in surface coverage during the transient, and is defined as the coverage differential parameter, $\Delta\Theta^{Trans}$, that is used in these studies. Notice that these calculations do not take into account the adsorption from the background gases between the points when the beam is turned on and when the flag is removed. This omission should not be critical, but it may explain, at least in part, the excess nitrogen seen in the transient in some cases: the absolute nitrogen production may be overestimated here because of the background term. The trends in the data are nevertheless expected to reflect the underlying surface chemistry of the reaction (see below).

Figure 10 displays the data that result from calculations such as those described in the previous paragraph for the nitrogen-coverage differential ($\Delta\Theta_N^{Trans}$) as a function of reaction temperature (a, left) and beam composition (b, right). There is a clear difference in behavior between the NO-rich (4:1 to 1:7) and CO-rich (1:15 to 1:99) beams. With NO-rich beams, $\Delta\Theta_N^{Trans}$ is negative at low temperatures because of the high value of the threshold nitrogen coverage needed for the steady-state reaction to start, it becomes positive at about 500−650 K because of the high rates of NO dissociation and subsequent

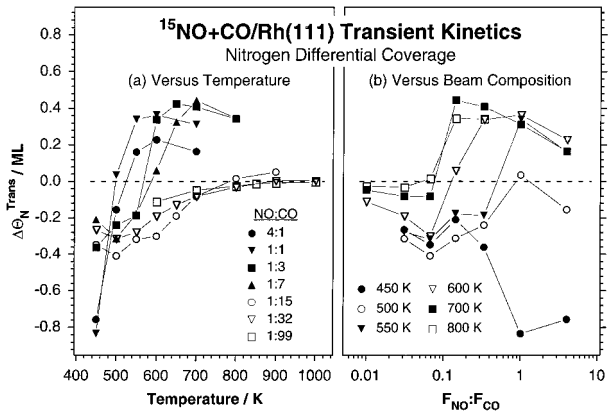

Figure 10. Transient nitrogen-coverage differential ($\Delta\Theta_N^{Trans}$) as a function of both temperature for different NO:CO beam compositions (a, left) and beam composition for different temperatures (b, right). There is a clear demarcation in behavior between NO-rich (4:1 to 1:7) and CO-rich (1:15 to 1:99) beams. The steady-state reaction rate reaches a maximum with all beam compositions when $\Delta\Theta_N^{Trans}$ is close to zero.

N_2 desorption under those conditions, and it decreases again at higher temperatures. With CO-rich beams, on the other hand, $\Delta\Theta_N^{Trans}$ is negative or close to zero at all temperatures. Recall that, in this regime, the surface becomes covered with CO first; NO then displaces the excess CO, but only over a long period of time, and asymptotically as the steady-state condition is approached. No overshooting in the N_2 production traces is seen with the CO-rich beams, except for the 1:15 NO:CO composition between 800 and 900 K. In general, the maximum in the steady-state rate for a given beam composition is reached at approximately the same temperature at which $\Delta\Theta_N^{Trans}$ becomes zero (the amount of N_2 produced in the transient matches that expected if there were no transient), or, more accurately, at the inflection point of the $\Delta\Theta_N^{Trans}$ versus temperature plots. These optimum temperatures are plotted in an Arrhenius form as a function of beam composition in Figure 4. Notice that these data follow reasonably closely those obtained from a determination of the conditions under which the steady state is reached rapidly and asymptotically.

A similar analysis was performed on the data for the CO_2 transient in order to extract information about the trends in oxygen surface coverage. Figure 11 displays the results obtained for the oxygen-coverage differential ($\Delta\Theta_O^{Trans}$) as a function of temperature for a number of beam compositions. Some important points about the behavior of the oxygen coverage in the transient are the following: (1) $\Delta\Theta_O^{Trans}$ is generally positive below 500 K, negative between 500 and 700 K, and close to zero above 700−800 K. (2) For a given beam composition, the minimum in $\Delta\Theta_O^{Trans}$, usually a large negative number, coincides with the optimum temperature for the steady-state process. (3) There is a general broadening in the temperature range in which $\Delta\Theta_O^{Trans}$ displays an appreciable negative value (relative to the minimum) as the beam becomes richer in CO. (4) The highest and lowest values of $\Delta\Theta_O^{Trans}$ are observed with the 1:3 NO:CO beam composition, at 400 and 550 K, respectively. (5) The variations in $\Delta\Theta_O^{Trans}$ as a function of temperature are less pronounced for both the CO-richest (1:99) and the NO-richest (4:1) beams. (6) Finally, as in the case of $\Delta\Theta_N^{Trans}$, the positive and negative values of $\Delta\Theta_O^{Trans}$ correspond to an overshooting of CO_2 production in the transient and a slow approach to the steady state, respectively.

3.7. Surface Coverages under Steady-State Reaction Conditions. As mentioned above, the transient behavior of the NO + CO reaction on Rh(111) can be correlated with that in

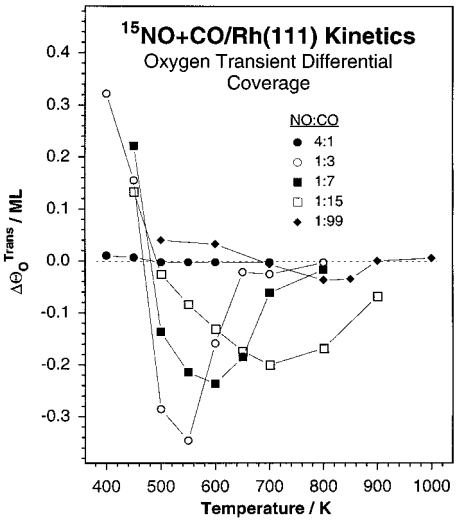

Figure 11. Transient oxygen-coverage differential ($\Delta\Theta_O^{Trans}$) as a function of temperature for different NO:CO beam compositions. Maximum steady-state rates are reached for large negative values of this parameter.

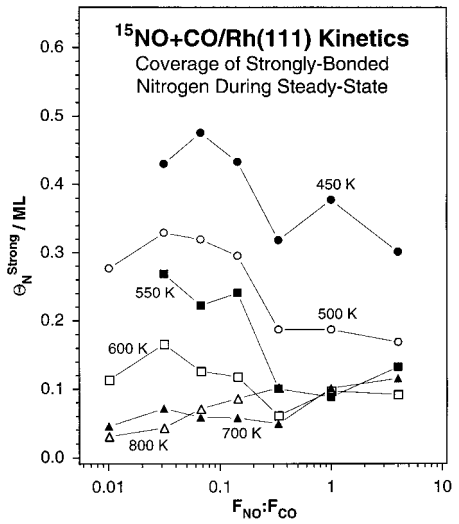

Figure 12. Coverages of strongly bonded nitrogen atoms under steady-state reaction conditions as a function of beam composition for a number of temperatures between 450 and 800 K. The coverage of this nitrogen decreases with temperature regardless of beam composition, and increases with CO concentration in the beam at most temperatures.

the steady-state catalytic regime. In particular, the delay in nitrogen production after turning the beam on is directly related to the buildup of a critical coverage of strongly bonded atomic nitrogen (Θ_N^{Strong}) on the surface.[3−5] The presence of such species was corroborated by TPD experiments performed at the end of the kinetic runs.[4,5] Figure 12 displays the coverage of this strongly bonded nitrogen as a function of beam composition for a number of reaction temperatures. One simple, general trend that is observed as a function of temperature is that the large coverages (close to 0.4 ML) seen at 450 K for all compositions decrease drastically above about 600 K. A small nitrogen-coverage increase is also observed with most beams above 700 K, after the coverage passes through a minimum value; a subsequent decrease to near zero monolayers then follows between 900 and 1000 K (data not shown here).[4] Θ_N^{Strong} is sensitive to the NO:CO ratio in the beam as well, generally increasing as the beam becomes richer in CO (at least at low temperatures), perhaps because of the increase in efficiency in the removal of surface oxygen by the CO.

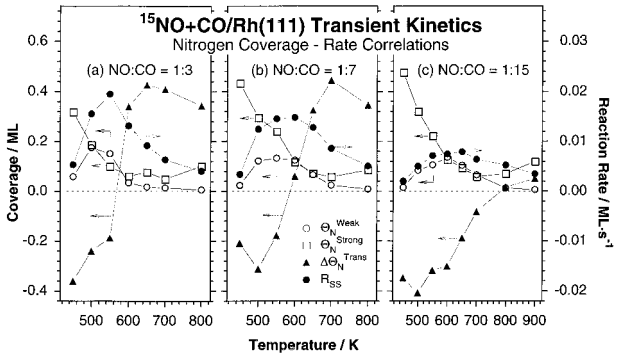

Figure 13. Weak (Θ_N^{Weak}, open circles) and strong (Θ_N^{Strong}, open squares) nitrogen coverages, transient nitrogen-coverage differential ($\Delta\Theta_N^{Trans}$, filled triangles), and steady-state rates (R_{ss}, filled circles) as a function of reaction temperature for 1:3 (a, left), 1:7 (b, middle), and 1:15 (c, right) NO:CO beam compositions. A direct correlation can be seen between the weak nitrogen coverage and the rate, and rate maxima for specific beam compositions are observed when $\Delta\Theta_N^{Trans} \cong 0$.

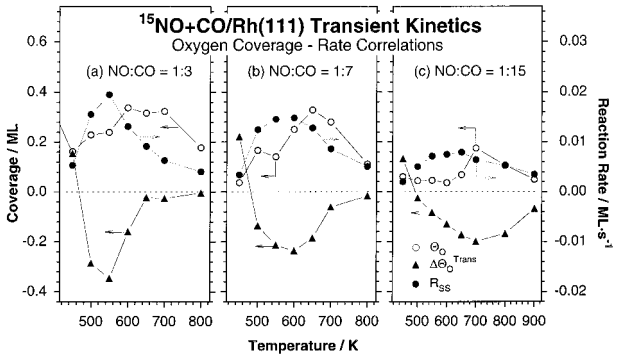

Figure 14. Oxygen coverage (Θ_O, open circles), transient oxygen-coverage differential ($\Delta\Theta_O^{Trans}$, filled triangles), and steady-state rates (R_{ss}, filled circles) for 1:3 (a, left), 1:7 (b, middle), and 1:15 (c, right) NO:CO beam compositions as a function of reaction temperature. A strong negative correlation can be seen between R_{ss} and $\Delta\Theta_O^{Trans}$.

A final comparison of the relevant parameters measured here for the (NO + CO)/Rh(111) system is presented in Figures 13 and 14. The dependencies of the coverages of strong (Θ_N^{Strong}) and labile (Θ_N^{Weak}) nitrogen in the steady state, as defined elsewhere,[4,5] are contrasted with the nitrogen-coverage transient differential ($\Delta\Theta_N^{Trans}$) defined in Figure 9 and the overall steady-state reaction rate (R_{ss}) as a function of temperature in Figure 13. Data were collected for three key beam compositions, namely, 1:3 (a, left), 1:7 (b, center), and 1:15 (c, right) NO:CO ratios. This figure shows the following: (1) The best direct correspondence is seen between steady-state reaction rates and Θ_N^{Weak}. (2) A more subtle correlation can also be identified between R_{ss} and $\Delta\Theta_N^{Trans}$, as $\Delta\Theta_N^{Trans}$ is roughly proportional to the negative of the derivative of R_{ss} with respect to temperature. (3) Maximum steady-state rates are observed when $\Delta\Theta_N^{Trans}$ is close to zero (or, more accurately, at the inflection point of the $\Delta\Theta_N^{Trans}$ versus temperature curves). (4) Θ_N^{Strong} generally decreases with reaction temperature, and is low (0.1 ML or less) by the time the maximum rates are reached. (5) There is an inverse correlation between $\Delta\Theta_N^{Trans}$ and Θ_N^{Strong}. Similar plots for R_{ss}, Θ_O, and $\Delta\Theta_O^{Trans}$ versus temperature (Figure 14) indicate that there is an approximately direct correlation between R_{ss} and Θ_O, although Θ_O generally peaks at higher temperatures than R_{ss}, and that there is a particularly good inverse correlation between R_{ss} and $\Delta\Theta_O^{Trans}$.

4. Discussion

4.1. Reaction Mechanism. The kinetic data for the transient of the reaction between NO and CO on Rh(111) surfaces presented here generally reinforce the conclusions reached from steady-state measurements on the same system.[4] To start, no evidence was obtained for the production of N_2O, either as an intermediate or as a desorption product in the transient (or in the steady state).[4,5] Perhaps more significant is the fact that the rate-limiting step in the transient often appears to be the production of N_2 molecules, the same as in the steady state. In connection with this result, it is useful to highlight the following few observations deriving from our experiments: (1) the almost immediate response of the rate of CO_2 production to the flag removal in the initial stage of the kinetic runs, (2) the slow kinetics of N_2 production seen below 700 K, (3) the need for the buildup of a critical nitrogen coverage on the surface before the start of the production of N_2, and (4) the inverse correlation between the threshold nitrogen coverage and the NO steady-state reduction rate.

Additional analysis of the transient kinetic data provides further support for the mechanism presented in our earlier report.[4] In the discussion of the results presented here it is important to remember that, as opposed to the case of the steady-state regime, the kinetics in the transient do not require that all the steps in the mechanism display equal rates. In other words, as the system goes from a clean metal surface at the beginning of the experiment to the steady state of the NO + CO reaction, both the surface concentrations and the rates of individual steps change in absolute as well as relative terms, hence the variations in rates over time seen in Figures 2 and 3. Observation of the transients suggests that molecular nitrogen production might be rate-limiting in most cases. Only with NO-rich mixtures or high temperatures is CO_2 formation slower than N_2 desorption.[4]

Another important aspect of the (NO + CO)/Rh system relevant to the discussion presented here is related to the dependence of the reaction rates on coverages. This dependence becomes evident by the product desorption patterns observed in the transients as the reaction approaches its steady state. A quick look at Figures 2 and 3 allows for the realization that there is an inverse correlation between the time evolution of the N_2 and CO_2 signals. Specifically, when one of the products, either CO_2 or N_2, forms at a high rate in the transient, the other displays a slow production rate. In general, at low temperatures, CO_2 production first peaks and then decreases toward its steady-state level, while nitrogen desorption increases slowly and reaches its steady state at a later time. This result means that, under those conditions, an excess of oxygen builds up on the surface at first; only after that Θ_O^{Excess} is removed (by the CO) can the atomic nitrogen that is required to reach the threshold value for molecular nitrogen production be deposited. Recall that, whereas NO dissociation is expected to deposit equimolar quantities of N and O on the surface in the initial stages of the NO + CO dosing, under steady-state conditions, the surface is covered almost exclusively with nitrogen. At high temperatures, in contrast, the CO_2 production increases slowly toward its steady state, while the N_2 production peaks within a few seconds of the removal of the flag from the beam path and then decreases towards its final steady-state level. The amount of nitrogen needed on the surface to trigger the N_2 desorption is small above 600 K, at which point N_2 formation is no longer rate-limiting. Despite the opposite behavior of the N_2 and CO_2 transients, however, the two products approach their steady-state levels simultaneously. This "180°-out-of-phase" evolution has previously been seen on Rh(110) by Comelli et al.,[10,40] and a related coverage dependence for the N_2 desorption rates from TPD studies on the NO/Rh(111) and N/Rh(111) systems has been reported by Belton et al.[30] Our observations suggest that the coverages of oxygen and nitrogen atoms are interrelated: the buildup of one species is often accomplished at the expense of the other. Repulsive interactions between N and O have in fact been inferred from a number of past studies.[3−5,14,15,20] In terms of the dependence of the transient on beam composition, the data in Figure 3 indicate that the high-temperature behavior is somewhat mimicked by NO-rich beams, while the low-temperature responses are paralleled by the runs with NO-lean beams. Composition-dependent reaction profiles at other temperatures (data not shown) support this analogy.

4.2. Initial Adsorption of NO and CO from Mixed NO + CO Beams. An important conclusion from the present work is the fact that the rates of NO and CO uptake on Rh(111) from NO + CO gas mixtures are affected in a significant way both by the composition of that mixture and by the presence of adsorbed species on the metal surface. For instance, Figure 5 clearly shows that the initial sticking probability of NO typically increases with NO:CO ratio and temperature. The changes in $s°_{NO}$ with temperature are particularly interesting, as they differ from our earlier studies for NO adsorption on clean Rh(111),[3] in which a temperature-independent response was seen below 800 K. This difference indicates that competition with CO alters the kinetics of NO adsorption. In general, $s°_{NO}$ in NO + CO mixtures is lower than that for pure NO (about 0.7), but it reaches a comparable value for close-to-stoichiometric (NO:CO = 1:3 to 1:7) mixtures and moderate (500−700 K) temperatures. A similar argument can be made for CO, for which the initial sticking coefficient is seen to decrease significantly above about 500 K. As mentioned in our previous reports,[4,5] the temperature dependence of the $s°_{NO}/s°_{CO}$ ratio could, in principle, provide an indication of the difference in adsorption barriers for the coadsorbed system, but, unfortunately, our data are too noisy for such calculations. Ultimately, $s°_{NO}$ and $s°_{CO}$ change only by a factor of 2−3 over the most relevant temperature range, and those changes account for a significant component of the variations in the overall NO + CO conversion rate in the steady-state regime only in the case of CO-rich beams. This fact is more clearly shown by the plots of $R_{ss}/s°_{NO}$ in Figure 7, which display essentially the same trends as those reported earlier for the steady-state rate.[4]

In contrast to the weak dependence that the reaction rates display on sticking coefficients, differences in adsorption energies between NO and CO on Rh(111) are of significance for the steady-state coverages and, as a consequence, for the steady-state rates. The adsorption of NO is clearly stronger than that of CO, as evidenced by the CO displacement shown in Figure 8. Assuming that optimum rates are reached with equimolar coverages of CO and NO on the surface, the variations in beam composition needed to reach the rate maximum at a given temperature reflect the differences in ΔH for CO and NO when coadsorbed on Rh(111). Analysis of the data in Figure 4 under that assumption indicates that the energy of adsorption of NO is approximately 11.5 ± 0.5 kcal/mol higher than that of CO. The adsorption energy of CO on clean Rh(111) has been reported to be about 35 kcal/mol,[44] but because NO does not desorb molecularly at low coverages (it dissociates instead),[3,14,28] no reliable value for its adsorption energy is available. On the basis of the arguments presented here, we estimate the latter energy to be slightly above 45 kcal/mol. This

difference in adsorption energies is the reason that the rate of NO + CO conversion reaches its maximum with slightly CO-rich beams.

4.3. Transient Behavior of Surface Coverages. One of the main premises of our discussion is that the behavior of the NO + CO system in the transient from the clean Rh(111) surface is directly related to the final steady-state condition of the reaction. This relationship is illustrated in a particularly clear way by the behavior of the parameters $\Delta\Theta_O^{Trans}$ and $\Delta\Theta_N^{Trans}$, defined in Figure 9, which is displayed in Figures 10 and 11. In particular, the value of $\Delta\Theta_O^{Trans}$ is positive and reaches a maximum below 450 K, but it becomes negative at higher temperatures except for the case of the 1:99 NO:CO beam, which shows positive values up to 600 K. It is clear from Figures 2 and 3 that, in most cases, CO_2 production is fast and approaches its steady state within the first 10−20 s after the molecular beam is turned on irrespective of temperature and beam composition. It can also be seen that, above 500 K, there is no longer any overshooting in the CO_2 production traces as in the cases below 500 K. Two important facts should be mentioned at this point. (1) Above 300 K, NO dissociates readily, at least at low and medium coverages,[28] and yields a 1:1 mixed layer of randomly adsorbed oxygen and ordered nitrogen islands on the rhodium surface.[45,46] (2) Oxygen removal by CO is severely impaired at high temperatures by the low residence time of CO on the surface,[4] hence the decrease in the overall steady-state rate of the NO + CO reaction. It is possible that, as the temperature is increased and the production of molecular nitrogen becomes faster, the ratio of oxygen to nitrogen on the surface increases, and the reaction becomes poisoned by the excess oxygen. On the other hand, at moderate temperatures oxygen might actually exert a beneficial effect on the overall reaction, helping in the formation of nitrogen molecules via the mutual repulsion between the surface N and O atoms. Also, an increase in the CO concentration in the beam facilitates the removal of the surface oxygen, but it does so only up to a point, because a large excess of CO poisons the reaction via CO blocking of active sites; higher temperatures render this step more inefficient as well. $\Delta\Theta_O^{Trans}$ appears to be an excellent parameter to reflect the appropriate balance among these counteracting effects, hence the inverse proportionality between R_{ss} and $\Delta\Theta_O^{Trans}$ seen in Figure 14.

In contrast to the case of $\Delta\Theta_O^{Trans}$, $\Delta\Theta_N^{Trans}$ is generally negative at low temperatures, and increases, often becoming positive, at high temperature. Clearly, the N_2 formation step becomes faster at higher temperatures, but also the threshold coverage of the strongly bonded nitrogen that is needed for the beginning of the N_2 production in the steady-state regime decreases with temperature. There are additional clear differences in the behavior of the $\Delta\Theta_N^{Trans}$ parameter between CO-rich and NO-rich beams. The faster oxygen removal by CO with CO-rich beams (1:15 to 1:99) generally increases the value of the nitrogen threshold coverage, hence the negative values (less than or equal to −0.1 ML) always seen for $\Delta\Theta_N^{Trans}$ from those mixtures. The low fluxes of NO in the CO-rich beams delay the buildup of surface nitrogen, as expected, but the lack of any overshooting in the rate of N_2 production in those cases can only be explained by the rapid removal of the coadsorbed oxygen. This is because, again, surface oxygen helps in the formation of molecular nitrogen; our previous work indicated that the rate of that reaction is roughly proportional to the combined N + O coverage, not just to Θ_N.[3] Above 700 K the critical nitrogen coverage needed to reach the steady state is low and, therefore, does not contribute significantly to $\Delta\Theta_N^{Trans}$, which approaches a value of zero.

The most salient feature in the behavior of $\Delta\Theta_N^{Trans}$ with NO-rich (4:1 to 1:7) beams is in the intermediate temperatures. High NO fluxes alone do not necessarily lead to maxima in $\Delta\Theta_N^{Trans}$. In fact, the maximum $\Delta\Theta_N^{Trans}$ value increases when going from NO:CO = 4:1 to NO:CO = 1:7 (although the temperature of this maximum changes as well, see Figure 10). This finding may again be attributed (at least in part) to the better cleaning of oxygen by the increasing CO concentration in the beam. High values of $\Delta\Theta_N^{Trans}$ mean that there is more surface nitrogen produced in the transient than expected on the basis of the steady-state behavior. As pointed out in the Results, such excess in N_2 production is, in part, a consequence of an experimental artifact, as some background adsorption does occur before the beginning of the experiment (the removal of the flag from the path of the beam). There is, however, an additional and perhaps more likely explanation for this behavior, namely, that the sticking coefficient of NO changes as the surface becomes covered with the adsorbates. As already discussed above, the sticking probability of NO on Rh(111) decreases when the adsorption of NO competes with that of CO. In NO-rich beams, in particular, this competition leads to an early excess of N deposition on the surface (via NO dissociation) and to the fast desorption of this nitrogen as N_2 a few seconds later (hence the overshooting in R_{N_2}) until the steady-state coverage is reached. Notice, however, that the deposition of N from fast NO adsorption and decomposition must be balanced by the removal of the oxygen byproduct, which requires the adsorption of significant amounts of CO as well. It is in this context that a zero value for $\Delta\Theta_N^{Trans}$ can be correlated with the optimum in the steady-state reaction rate, because $\Delta\Theta_N^{Trans} = 0$ corresponds to conditions under which the surface concentrations of NO and CO are stoichiometric.

The correlations between the different nitrogen (Θ_N^{Strong}, Θ_N^{Weak}, and $\Delta\Theta_N^{Trans}$) and oxygen (Θ_O and $\Delta\Theta_O^{Trans}$) coverages and the steady-state rates (shown in Figures 13 and 14) can be used to explain most of the overall trends in the NO + CO reaction. It is to be emphasized that the behavior of the NO + CO reaction rate at any specific composition and temperature is the consequence of what happens during the transient state. For example, the inflection points in the plots of $\Delta\Theta_N^{Trans}$ versus temperature correlate well with the final rates, and the high positive values of $\Delta\Theta_N^{Trans}$ found with NO-rich beams at intermediate temperatures are associated with low Θ_N^{Strong} ($\leq$0.1 ML). There is an additional direct correlation between reaction rates and Θ_N^{Weak} which has been discussed in detail elsewhere.[5,6] In terms of oxygen coverages, high negative values of $\Delta\Theta_O^{Trans}$ in the transient correspond to high steady-state rates for all beam compositions. There is an additional, approximately inverse correlation between Θ_O and $\Delta\Theta_O^{Trans}$, at least with NO-rich beams (1:3 and 1:7 NO:CO compositions): Θ_O increases with temperature up to some intermediate point and then decreases again, whereas $\Delta\Theta_O^{Trans}$ decreases at first and then regains some of its low-temperature value. Finally, there is an important connection between $\Delta\Theta_N^{Trans}$ and $\Delta\Theta_O^{Trans}$, as those two quantities change in somewhat opposite ways with changing temperature; this last correlation points to the redox nature of the NO + CO reaction.

5. Conclusions

This paper reports results from a kinetic study on the transient of the NO + CO conversion on a Rh(111) single crystal in going

from a clean metal surface to its steady state under a wide range of NO:CO ratios and temperatures. The experiments were carried out isothermally and under ultrahigh vacuum by using effusive collimated beams, but they were performed under conditions such that the NO reduction could be sustained in a catalytic regime similar to that encountered in realistic catalytic converters. As in the steady-state regime,[4] it was seen here that in the transient there is an optimum reaction temperature for a given NO + CO beam composition that maximizes the overall behavior of the system in terms of leading to the steady-state regime after a short delay. This is manifested primarily by an almost asymptotic approach to the steady-state level without significant deviations in either CO_2 or N_2 production rates from their final values, and also by a balance in the amounts of atomic N and O deposited on the surface in the transient. The maximum in the steady-state reaction rate shifts to higher temperatures with increasing CO concentration in the reaction mixture, that is, there is an optimum NO:CO ratio that maximizes the overall rate at a given temperature and that changes with varying surface temperature. This synergy is such that it leads to approximately stoichiometric mixtures of the reactants on the surface at the reaction rate maxima. Significant deviations from the optimum rates are observed when the reaction is carried out under extreme conditions. High initial rates for N_2 production are observed on the high-temperature side, at least with all NO-rich beam compositions (4:1 to 1:7). Conversely, CO_2 production is favored for all beam compositions on the low-temperature side, below 500 K, presumably because of the efficiency with which CO reacts with surface oxygen under those conditions.

The depositions of oxygen and nitrogen on the surface in the initial stages of the reaction reflect well the general trends seen for the steady-state NO + CO conversion rates. Whenever the transient coverages of N or O exceed those expected on the basis of the steady-state rates, the final rate of reaction is slow; the maximum rates are attained when $\Delta\Theta_N^{Trans}$ is approximately zero. The coverages of nitrogen and oxygen atoms are mutually interactive, so an excess of one usually precludes the buildup of the other. Differences in the relative coverages of NO and CO on the surface in comparison with the relative NO and CO compositions of the impinging beams (which are due to differences in the relative rates for adsorption and desorption of those species on the surface) are also related to the steady-state rates. Variations in surface coverages due to differences in adsorption energies are, in fact, one of the main reasons that explain the steady-state catalytic behavior of this system. NO was found to adsorb preferentially when competing with CO. This preference becomes more acute at higher temperatures, as manifested by an increase in the sticking coefficient of NO and a corresponding decrease in that of CO, and by an adsorption energy difference of about 11.5 kcal/mol. An extreme manifestation of this phenomenon is the displacement of adsorbed CO by NO from Rh(111) surfaces that was observed between 400 and 500 K with all beam compositions and at high temperatures in a few selected instances. The changes in $s°_{NO}$ and $s°_{CO}$, on the other hand, are not critical for determining the steady-state NO + CO reaction rates.

Acknowledgment. Funding for this research was provided by a grant from the National Science Foundation (CTS-9812760).

References and Notes

(1) Imbihl, R.; Ertl, G. *Chem. Rev.* **1995**, *95*, 697.
(2) Cobden, P. D.; Nieuwenhuys, B. E.; Esch, F.; Baraldi, A.; Comelli, G.; Lizzit, S.; Kiskinova, M. *Surf. Sci.* **1998**, *416*, 264.
(3) Aryafar, M.; Zaera, F. *J. Catal.* **1998**, *175*, 316.
(4) Gopinath, C. S.; Zaera, F. *J. Catal.* **1999**, *186*, 387.
(5) Zaera, F.; Gopinath, C. S. *J. Chem. Phys.* **1999**, *111*, 8088.
(6) Zaera, F.; Gopinath, C. S. In preparation.
(7) Taylor, K. C. *Catal. Rev. Sci. Eng.* **1993**, *35*, 457.
(8) Shelef, M.; Graham, G. W. *Catal. Rev. Sci. Eng.* **1994**, *36*, 433.
(9) Zhdanov, V. P.; Kasemo, B. *Surf. Sci. Rep.* **1997**, *29*, 31.
(10) Comelli, G.; Dhanak, V. R.; Kiskinova, M.; Prince, K. C.; Rosei, R. *Surf. Sci. Rep.* **1998**, *32*, 165.
(11) Campbell, C. T.; White, J. M. *Appl. Surf. Sci.* **1978**, *1*, 347.
(12) Dubois, L. H.; Hansma, P. K.; Somorjai, G. A. *J. Catal.* **1980**, *65*, 318.
(13) Becker, W. C.; Bell, A. T. *J. Catal.* **1983**, *84*, 200.
(14) Root, T. W.; Schmidt, L. D.; Fisher, G. B. *Surf. Sci.* **1983**, *134*, 30.
(15) Root, T. W.; Schmidt, L. D.; Fisher, G. B. *Surf. Sci.* **1985**, *150*, 173.
(16) DeLouise, L. A.; Winograd, N. *Surf. Sci.* **1985**, *159*, 199.
(17) Oh, S. H.; Carpenter, J. E. *J. Catal.* **1986**, *101*, 114.
(18) Hendershot, R. E.; Hansen, R. S. *J. Catal.* **1986**, *98*, 150.
(19) Root, T. W.; Fisher, G. B.; Schmidt, L. D. *J. Chem. Phys.* **1986**, *85*, 4679.
(20) Root, T. W.; Fisher, G. B.; Schmidt, L. D. *J. Chem. Phys.* **1986**, *85*, 4687.
(21) Oh, S. H.; Fisher, G. B.; Carpenter, J. E.; Goodman, D. W. *J. Catal.* **1986**, *100*, 360.
(22) Schwartz, S. B.; Fisher, G. B.; Schmidt, L. D. *J. Phys. Chem.* **1988**, *92*, 389.
(23) Peden, C. H. F.; Goodman, D. W.; Blair, D. S.; Berlowitz, P. J.; Fisher, G. B.; Oh, S. H. *J. Phys. Chem.* **1988**, *92*, 1563.
(24) Kao, C.-T.; Blackman, G. S.; Van Hove, M. A.; Somorjai, G. A.; Chan, C.-M. *Surf. Sci.* **1989**, *224*, 77.
(25) Cho, B. K.; Shanks, B. H.; Bailey, J. E. *J. Catal.* **1989**, *115*, 486.
(26) Oh, S. H. *J. Catal.* **1990**, *124*, 477.
(27) Bugyi, L.; Solymosi, F. *Surf. Sci.* **1991**, *258*, 55.
(28) Borg, H. J.; Reijerse, J. F. C.-J. M.; van Santen, R. A.; Niemantsverdriet, J. W. *J. Chem. Phys.* **1994**, *101*, 10052.
(29) Cho, B. K. *J. Catal.* **1994**, *148*, 697.
(30) Belton, D. N.; DiMaggio, C. L.; Ng, K. Y. S. *J. Catal.* **1993**, *144*, 273.
(31) Belton, D. N.; Schmieg, S. J. *J. Catal.* **1993**, *144*, 9.
(32) Ng, K. Y. S.; Belton, D. N.; Schmieg, S. J.; Fisher, G. B. *J. Catal.* **1994**, *146*, 394.
(33) Peden, C. H. F.; Belton, D. N.; Schmieg, S. J. *J. Catal.* **1995**, *155*, 204.
(34) Belton, D. N.; DiMaggio, C. L.; Schmieg, S. J.; Ng, K. Y. S. *J. Catal.* **1995**, *157*, 559.
(35) Permana, H.; Ng, K. Y. S.; Peden, C. H. F.; Schmieg, S. J.; Lambert, D. K.; Belton, D. N. *J. Catal.* **1996**, *164*, 194.
(36) Liu, J.; Xu, M.; Nordmeyer, T.; Zaera, F. *J. Phys. Chem.* **1995**, *99*, 6167.
(37) Öfner, H.; Zaera, F. *J. Phys. Chem.* **1997**, *101*, 396.
(38) *Vacuum Physics and Technology*; Weissler, G. L., Carlson, R. W., Eds.; Academic Press: New York, 1979.
(39) Zaera, F.; Liu, J.; Xu, M. *J. Chem. Phys.* **1997**, *106*, 4204.
(40) Baraldi, A.; Dhanak, V. R.; Comelli, G.; Kiskinova, M.; Rosei, R. *Appl. Surf. Sci.* **1993**, *68*, 395.
(41) Yamada, T.; Onishi, T.; Tamaru, K. *Surf. Sci.* **1983**, *133*, 533.
(42) Shen, S.; Zaera, F.; Fischer, D. A.; Gland, J. L. *J. Chem. Phys.* **1988**, *89*, 590.
(43) Gland, J. L.; Fischer, D. A.; Shen, S.; Zaera, F. *J. Am. Chem. Soc.* **1990**, *112*, 5695.
(44) Thiel, P. A.; Williams, E. D.; Yates, J. T., Jr.; Weinberg, W. H. *Surf. Sci.* **1979**, *84*, 54.
(45) Murray, P. W.; Thornton, G.; Bowker, M.; Dhanak, V. R.; Baraldi, A.; Rosei, R.; Kiskinova, M. *Phys. Rev. Lett.* **1993**, *26*, 4369.
(46) Xu, H.; Ng, K. Y. S. *Surf. Sci.* **1996**, *365*, 779.